# Feasible Kinematic Sensitivity in Cable Robots Based on Interval Analysis

S. A. Khalilpour, A. Zarif Loloei, H. D. Taghirad, and M. Tale Masouleh

**Abstract** The kinematic sensitivity has been recently proposed as a unit-consistent performance index to circumvent several shortcomings of some notorious indices such as dexterity. This paper presents a systematic interval approach for computing an index by which two important kinematic properties, namely feasible workspace and kinematic sensitivity, are blended into each other. The proposed index may be used to efficiently design different parallel mechanisms, and cable driven robots. By this measure, and for parallel manipulators, it is possible to visualize constant orientation workspace of the mechanism where the kinematic sensitivity is less than a desired value considered by the designer. For cable driven redundant robots, the controllable workspace is combined with the desired kinematic sensitivity property, to determine the so-called feasible kinematic sensitivity workspace of the robot. Three case studies is considered for the development of the idea and verification of the results, through which a conventional planar parallel manipulator, a redundant one and a cable driven robot is examined in detail. Finally, the paper provides some hints for the optimum design of the mechanisms under study by introducing the concept of minimum feasible kinematic sensitivity covering the whole workspace.

## 1 Introduction

Cable driven redundant parallel manipulators (CDRPMs) consist of a moving platform which is connected by the means of actuated cables to the base. Redundancy

S. A. Khalilpour, A. Zarif Loloei, and H. D. Taghirad
Advanced Robotics and Automated Systems, Faculty of Electrical and Computer Engineering, K.N. Toosi University of Technology, P.O. Box 16315-1355, Tehran, lran e-mail: khalilpour, zarif, taghirad@kntu.ac.ir

Mehdi Tale Masouleh
Faculty of Modern Science and New Technology, University of Tehran, Tehran, Iran, e-mail: mehdi.tale-masouleh.1@ulaval.ca

is an inherent requirement for CDRPMs due to the fact that cables can only pull but cannot push the moving platform. Thus, in a non-singular posture, the moving platform can perform $n$ Degree-Of-Freedom (DOF) provided that at least $n+1$ cables are used. CDRPMs are special design of parallel manipulators (PMs) that heritage the advantages of PMs such as high acceleration and high load carrying capability and at the same time, have alleviated some of their shortcomings, such as restricted workspace. Due to the several eminent features of CDRPMs, they have stimulated the interest of many researchers and they are becoming the state-of-the-art in many real applications, such as telescope [24], haptic interface [3], motion trackers [6], rescue robotics [25], metrology [27], rehabilitation [18], sport training [16], heavy load transportation [9] and surgery [7]. However there are still some gap to fill in the kinematic properties of such mechanisms, such as workspace and kinematic sensitivity, which is the concerns of this paper.

The workspace of CDRPM are investigated upon different perspectives and different types of workspace are proposed in the literature. In short, four different types of workspace have been introduced: (1) Wrench feasible workspace [4], (2) Dynamic workspace [1], (3) Static workspace [5] and (4) Controllable workspace [26]. In this paper, more emphasis is placed on the controllable workspace which represents the most general feasible workspace. Controllable workspace pertains at finding the set of poses (position and orientation) of the moving platform in which any wrench can be generated by the moving platform while cables are all in tension.

Extensive presence of singular points in PMs and the challenge to obtain and avoid them is one of the major drawbacks of this kind of mechanisms. In the design of PMs, usually kinematics performance indices are used to reduce the singularities and to improve the performance of the mechanism under study. Most popular indices are Yoshikawa manipulability [28] and the dexterity indices [23], which entail some limits and as stated in [2], seems to have not drawn a consensus among the robotics community. The latter problem relies on the impossibility to define a single invariant metric for the special Euclidean group, i.e., the Jacobian matrices are nonhomogeneous. To circumvent the latter problem, recently two different indices named point-displacement and rotational kinematic sensitivities are proposed which their meaning is thought to be clear and definite to the designer of a robotic manipulator [21]. These indices provide tight upper bounds on the magnitudes of the end-effector rotations and point-displacements, respectively under a unit-magnitude array of actuated-joint displacement [20].

The kinematic analysis of PMs require a suitable framework in order to propose a proper and systematic method. The mathematical framework of this paper is based on interval analysis [14], using the intlab package [19]. There are host of advantages relevant to using interval analysis as an alternative numerical method in order to obtain practically competent results for the analysis of kinematic properties of robotics mechanical systems [8]. In this paper our intrench toward applying interval analysis to the kinematic analysis can be summarized as follows [12]: (1) In contrast to many other intelligent mathematical tools which would result in a lengthy computation process and may converge to a local optimum, interval analysis is not a *black box*, since it requires to combine heuristics and numerical concepts to make it more

effective, (2) It allows to find all the solutions with inequalities within a given search space [13, 17] (3) For two and three-dimensional problem one can see the evolution of the solutions and to monitor the procedure in order to have better insight into the problem, (4) it allows to take into account uncertainties in the model of the robot and (5) For the problem in which infinity norm are involved, interval analysis may solve the problem more efficiently rather than other methods since infinity norm is a non-analytical function and consequently mathematical operations are not tractable.

This paper aims at introducing a more practical workspace for the CDRPMs in which the kinematic sensitivity is also taken into account while computing the controllable workspace. To this end, upon blending these two concepts, a new workspace is introduced which is referred to as *Feasible Kinematic Sensitivity* (FKS) and can be also regarded as a performance index. FKS pertains at finding a part of controllable workspace in which the kinematic sensitivity is less that a desired value. As it is the case for kinematic sensitivity and controllable workspace, the mathematical framework to obtain FKS is based on interval analysis and, to do so, a systematic approach is proposed.

The remainder of this paper is organized as follows. First, interval analysis is reviewed and the general concepts are introduced. Then based on the work presented in [20], the general idea of kinematic sensitivity is reviewed. The paper follows by exploring the concept of kinematic sensitivity by means of interval analysis upon proposing some systematic algorithms where it is applied to 3-R$\underline{P}$R PM and 4-R$\underline{P}$R redundant PM. Then the interval formulation of the controllable workspace is investigated for 3-DOFs CDRPMs with four cables. As the central subject of this paper, feasible kinematic sensitivity workspace is introduced and examined for the case studies. Finally, the paper concludes with some remarks to provide some insight to the optimum synthesis of CDRPMs.

## 2 Background Materials

### *2.1 Interval Analysis*

Interval analysis is amongst the numerical methods proposed in the literature that allows to safely solve the problem, and to obtain a guaranteed result. The basic principles of interval analysis are simple, where efficient implementation requires a high expertise level. In interval analysis, one deals with intervals of numbers instead of the numbers themselves [14]:

$$[x] = [\underline{x}, \bar{x}] = \{x | x \in R, \underline{x} \leq x \leq \bar{x}\} \tag{1}$$

where $\underline{x}$ is the left endpoint and $\bar{x}$ is the right endpoint of the interval. By an $n$-dimensional interval vector, we mean an ordered n-tuple of intervals:

$$\mathbf{X} = (X_1, \ldots, X_n) \tag{2}$$

In interval analysis all variables are independently investigated [15]. Thus the output range of interval function could be wider than the function span, but certainly the answer region lies within the output range. Therefore applying interval analysis has its own difficulties, but on the other hand the answer it gives is guaranteed, meaning that negligible errors that result from mathematical operations such as rounding and estimation, are not present. In this paper, interval analysis is not introduced in detail, since it is beyond the scope of this study and reader are referred to [11, 15] for a more comprehensive detail. It should be noted that all the interval algorithms proposed in this paper are implemented in Matlab which uses the INTLAB package supporting interval calculations.

### *2.2 Kinematic Sensitivity Indices*

Kinematic sensitivity is defined as the maximum error that occurs in the Cartesian workspace as a result of bounded errors in the joint space ($\|\rho\| \leq 1$). In order to obtain consistent unit indices, two indices have been defined in [2]:

$$\sigma_{r_c,f} \equiv \max_{\|\boldsymbol{\rho}\|_c=1} \|\boldsymbol{\phi}\|_f \qquad \text{and} \qquad \sigma_{p_c,f} \equiv \max_{\|\boldsymbol{\rho}\|_c=1} \|\mathbf{p}\|_f \tag{3}$$

in which, $\rho \in \mathbb{R}^n$ represents small actuator displacements and $x = [\mathbf{p}, \phi]$ stands for the pose of the end-effector. Moreover, $c = \{2, \infty\}$ and $f = \{2, \infty\}$ are respectively the types of norm for which the constraint and the objective are expressed. From the results obtained from [20], it can be inferred that two situations may correctly represent the kinematic sensitivity, which will be used for the purposes of this paper: (1) The constraint and objective functions are both expressed using $\infty$-norms ($c = f = \infty$) and (2) The constraint and objective functions are expressed respectively with $\infty$ and 2-norms ($c = \infty$, $f = 2$).

## 3 Investigation of Kinematic Sensitivity of Non-redundant Planar Parallel Mechanisms

This section is devoted entirely to an overview on the computation of the kinematic sensitivity of non-redundant planar PMs based on the results reported in [21, 22, 20] and, as a case study, the so-called 3-R$\underline{\text{P}}$R is considered[1]. As pointed out previously, the two different situations explained above, i.e., ($c = f = \infty$ and $c = \infty$ and $f = 2$), are considered for computing the kinematic sensitivity. Although the concepts presented in this section is to the majority of intents and purposes the same as the one presented in [20], it provides for the first time, the framework to compute the kine-

[1] Here and throughout this paper, R and P stands respectively for a revolute and prismatic joint where the underlined joint is actuated.

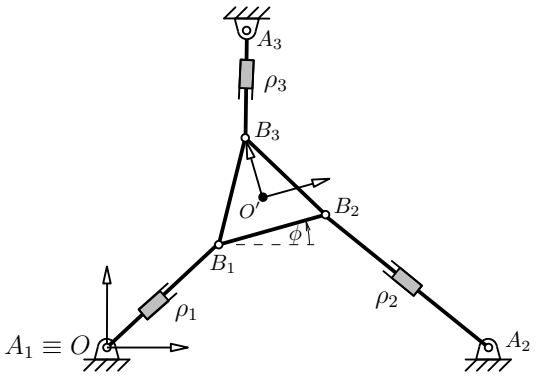


**Fig. 1** A 3-RPR parallel manipulator. Taken from [20].

matic sensitivity by using interval analysis. More specifically, the main objective of this section is to lay down the essential for the rest of the paper by introducing an interval-based algorithm which leads to obtain a region within the workspace of the mechanism, referred to as *feasible kinematic sensitivity workspace*, where the kinematic sensitivity is less than a given value, $\sigma_d$. It is worth noting that the computation of the constant-orientation workspace, reachable area of the moving platform for a given orientation of the moving platform and given stroke of actuator, is integrated in the proposed algorithm. As a geometrical point of view, the constant-orientation workspace of a 3-RPR PM can be made equivalent to the intersection of six circles, arisen from the minimum and maximum stroke of the prismatic actuators. This can be readily obtained using interval analysis and due to its simplicity, the details of such calculations are skipped in this paper. Furthermore, here and throughout this paper, for the sake of simplicity, the constant-orientation workspace is referred to as workspace.

Figure 1 represents schematically a 3-RPR parallel manipulator performing 3-DOF where the pose of the end-effector is denoted by $(x, y, \phi)$. Both fixed and moving platforms are considered as equilateral triangles that are encompassed by circles with radius 1 and 5, respectively, where the center of each triangle is coincidence on the circumambient circles centers. As it will be discussed latter on, from the results presented in [10] having equilateral triangles for the fixed base and moving platform results in a circle for the singularity curve which considerably optimizes the singularity-free workspace and is a definite asset in the practice. The Jacobian matrix, $\mathbf{K}$, with respect to the pose of the mechanism, $(x, y, \phi)$, may be written in an interval form, $[\mathbf{K}]$, as:

$$[\mathbf{K}] = \mathbf{K}([x], [y], [\phi]), \qquad \mathbf{K} = \begin{bmatrix} n_{1x} & n_{1y} & (\mathbf{b}_1 \times \mathbf{n}_1) \cdot \mathbf{k} \\ n_{2x} & n_{2y} & (\mathbf{b}_2 \times \mathbf{n}_2) \cdot \mathbf{k} \\ n_{3x} & n_{3y} & (\mathbf{b}_3 \times \mathbf{n}_3) \cdot \mathbf{k} \end{bmatrix} \tag{4}$$

In the above, $\mathbf{b}_i$, $i = 1, 2, 3$, denotes the position vector of point $B_i$ in the fixed frame, and the unit vector along the $i^{\text{th}}$ prismatic joint direction is denoted by

**Table 1** Pseudo-code for the calculation of the interval vertices of the polyhedron in a non-redundant parallel manipulator.

*Function:* Compute-Vertex-Nonredundant([K])

```
t=1
for i1=1:2
   for i2=1:2
   ⋮
      for i_{m-1}=1:2
         [temp]=[1,(-1)^{i1},(-1)^{i2},...,(-1)^{i_{m-1}}]^T
         [Vertices(t)]=verifylss([K],[temp])
         t=t+1
      end
   ⋮
   end
end
```

$\mathbf{n}_i = [n_{i_x}, n_{i_y}, 0]^T$. For a more comprehensive information regarding the kinematic properties of these kind of PMs, readers are referred to [22, 20].

## *3.1 Kinematic Sensitivity with ∞-norms on Constraint and Objective Function*

In this case, since dealing with $c = \infty$ for the constraint, the constraint inequality $\|\rho\|_\infty \leq 1$ can be replaced by $\|\mathbf{Kx}\|_\infty \leq 1$, from the Jacobian relation. Inequality $\|\mathbf{Kx}\|_\infty \leq 1$ stands for a polyhedron with $2^n$ vertices in $\mathbb{R}^n$ where $n$ represents the DOF of the PMs under study. The first step toward calculating the kinematic sensitivity for both ∞– or 2–norm consists of obtaining the vertices of the latter polyhedron, which can be done by solving the inequality $[\mathbf{K} \ -\mathbf{K}^T] \leq \mathbf{1}$. By using interval formulation of the Jacobian matrix, the intervals in which each vertices of the polyhedron is bounded, can be computed. Therefore the combination of all the interval vertices leads to interval formulation of the polyhedron. From the fact that the polyhedrons are symmetric with respect to the origin, calculation of half of them is sufficient. The pseudo-codes given in Table 1, provides the logic in changing the intervals of these vertices. Note that, the function `verifylss`$([A],[B])$ in the pseudo-codes given in Table 1 is a function of intlab toolbox that solves the system of equations $[A].[X] = [B]$, in which $[A]$ and $[B]$ are interval matrices and $[X]$ is a interval vector.

In the case of a 3-RPR PM, the number of vertices of the hexahedron is $2^3 = 8$ and because of being symmetric the calculation of four vertices is sufficient. As a geometric stand point, in this case, using interval analysis to calculate the kinematic sensitivity can be made equivalent to the map of the vertices to a cube that their

**Table 2** The proposed pseudo-code for the calculations of minimum and maximum kinematic sensitivity in the workspace.

***Input***:$([x_t],[y_t],\phi,\varepsilon,\sigma_d)$
***Output***: $(L_{in},L_{out},L_{neg})$

```
L ← ([x_t],[y_t])
while L ≠ ∅
   [K]=Compute-Jacobian-Matrix([X],[Y],φ)
   [V]=Compute-Vertex-non-redundant([K])
  if Feasible ([V],σ_d) then
      L_in ← ([X],[Y])
  else if Out([V],σ_d) then
      L_out ← ([X],[Y])
  else if size([X],[Y]) ≥ ε then
      L ← Bisect ([X],[Y])
   else
      L_neg ← ([X],[Y])
   end if
end while
```

dimensions in all the Cartesian directions are equal to the width of the calculated interval of the corresponding vertex. Re-formulating the relations obtained in [20] for the point-displacement and rotational kinematic sensitivities, when $c = f = \infty$, for a given position in the specified interval in the direction of the pose of the mechanism, leads to the following for the maximum point-displacement and rotational kinematic sensitivities:

$$\max \sigma_{p_{\infty,\infty}} = \max_{i=1,\ldots,4} (\mathrm{mag}([X_i]), \mathrm{mag}([Y_i])) \tag{5}$$

$$\max \sigma_{\phi_{\infty,\infty}} = \max_{i=1,\ldots,4} (\mathrm{mag}([\phi_i])) \tag{6}$$

where $\mathrm{mag}(\cdot)$ for its interval argument computes the distance of the farthest point in the interval from the coordinates origin. Furthermore, $X_i, Y_i, \phi_i$ constitute the elements of the vectors [Vertices(t)] obtained from the pseudo-code presented in Table 1. Similarly, the minimum kinematic sensitivity of the inner points of the interval is also calculated by:

$$\min \sigma_{p_{\infty,\infty}} = \max_{i=1,\ldots,4} (\mathrm{mig}([X_i]), \mathrm{mig}([Y_i])) \tag{7}$$

$$\min \sigma_{\phi_{\infty,\infty}} = \max_{i=1,\ldots,4} (\mathrm{mig}([\phi_i])) \tag{8}$$

where $\mathrm{mig}(\cdot)$ for its interval argument stands for the distance of the nearest point in the interval from the coordinates origin.

Table 2 provides the pseudo-code describing the interval formulation to obtain the maximum and minimum kinematic sensitivity, Eqs. (5-8), where $[x_t]$ and $[y_t]$ stands for the workspace of the mechanism, $L_{\mathrm{in}}$ and $L_{\mathrm{out}}$ represent the desired and

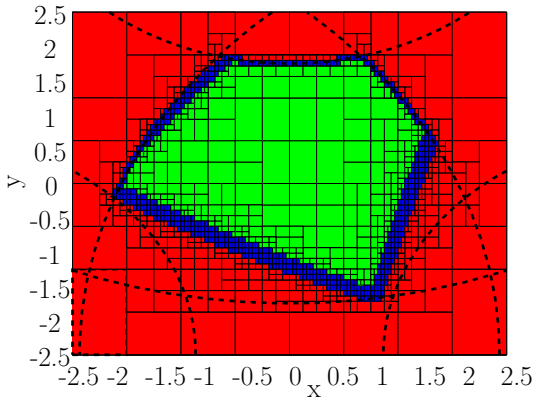


**Fig. 2** Point-displacement FKS, the inside (green) region, of a 3-RPR PM with $c = f = \infty$ and $\sigma_d = 0.35$ for $\phi = 45$. The dashed lines represent the boundary of the workspace.

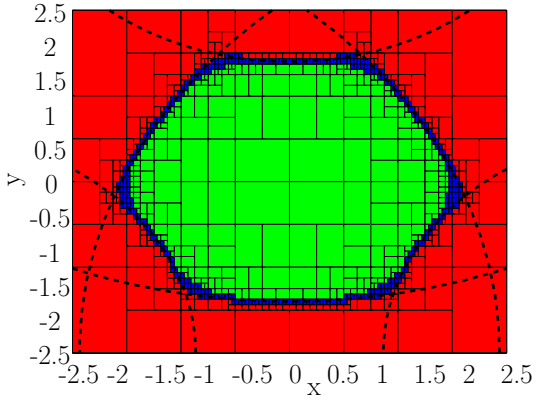


**Fig. 3** Rotational FKS, the inside (green) region, of a 3-RPR PM with $c = f = \infty$ and $\sigma_d = 0.35$ for $\phi = 45$. The dashed lines represent the boundary of the workspace.

undesired intervals of the workspace regarding to the criteria fixed for the kinematic sensitivity, $\sigma_d$, respectively. Moreover, $L_{\text{neg}}$ involves the bound intervals, calculated according to the $\varepsilon$ value. If the maximum value of kinematic sensitivity in the related interval is less than the desired value, $\sigma_d$, the interval is certainly inside the desired region and the function feasible $([V], \sigma_d)$ will return a value as one. Moreover, if the minimum value of kinematic sensitivity in the related interval is certainly more than the desired value, the interval is out of the desired region and the function out $([V], \sigma_d)$ will be activated. In the case that the workspace of the end-effector is not sufficiently small for the kinematic sensitivity of the points to have a similar behavior, the region should be split up into two intervals, in order that in the new intervals one of the functions feasible$([V], \sigma_d)$ or out$([V], \sigma_d)$ becomes active. The interval bisecting sequence pursues to the points that the remained intervals becomes small enough with respect to $\varepsilon$.

Figures 2 and 3 represent respectively the point-displacement and rotational kinematic sensitivity upon applying Eq. (5-8) and the pseudo-code presented in Table 2 for a given orientation of the moving platform, $\phi = \frac{\pi}{4}$. In the latter figures, the inside (green) region indicates a region that the 3-RPR robot of Fig. 1 has a kinematic

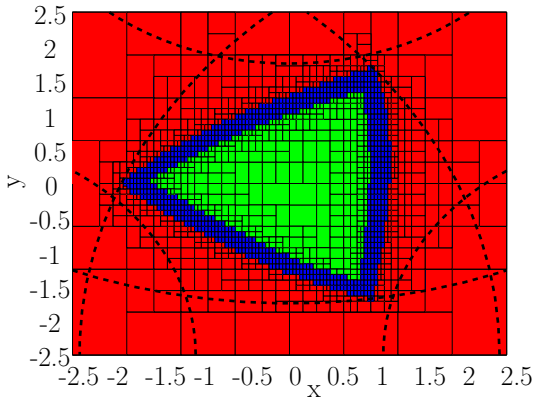


**Fig. 4** Point displacement FKS, the inside (green) region, of a 3-RPR PM with $c = \infty$, $f = 2$ and $\sigma_d = 0.35$ for $\phi = 45$. The dashed lines represent the boundary of the workspace.

sensitivity less than 0.35 and the outside (red) region, corresponds to the region corresponding to more than 0.35. As it can be observed outside (red) region is separated by the dark (blue) boxes from the inside (green) one which means that interval analysis was not able to reach to a conclusion for these boxes. These boxes represent the boundary of the FKS and it could be small as possible upon increasing the iteration. From the results obtained in [10], since the fixed and moving frame are equilateral, it can be also confirmed that the singularity curve is a circle centers at $(0,0)$ with a radius of 4.3507 for the 3-RPR PM under study. As it can deduced form Fig. 3, the green region is inside the singularity circle and consequently is singularity-free. This leads to have a conservative but safer constant-orientation workspace which is singularity-free.

## *3.2 Kinematic Sensitivity with ∞-norm for the Constraint and 2-norm for the Objective Function*

As aforementioned, for the calculation of the maximum and minimum of the kinematic sensitivity for this case, i.e., $c = 2$ and $f = \infty$, one should find the vertices of the polyhedron which was fully described in the previous section. From the results presented in [20], the kinematic sensitivity for $c = 2$ and $f = \infty$ in the interval form can be formulated as follows:

$$\max \sigma_{p_{\infty,2}} = \max_{i=1,\ldots,4} (\mathrm{mag}(\sqrt{{X_i}^2 + {Y_i}^2})) \tag{9}$$

$$\min \sigma_{p_{\infty,2}} = \max_{i=1,\ldots,4} (\mathrm{mig}(\sqrt{{X_i}^2 + {Y_i}^2})) \tag{10}$$

In this specific PM where the mechanisms performs only one rotational DOF then the rotational kinematic sensitivity with infinity- and two-norm are identical. Figure 4 illustrates the point-displacement FKS, where $\sigma_d$ is less than 0.35.

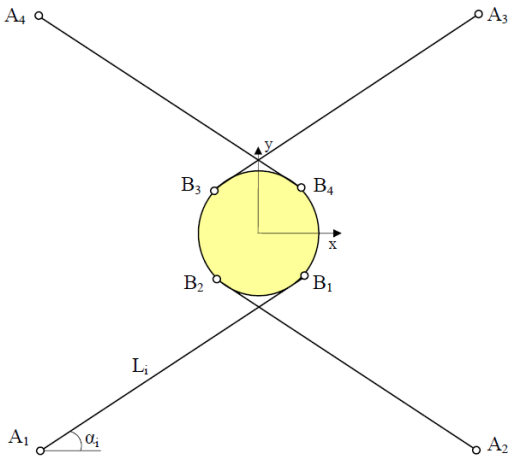


**Fig. 5** A 4-RPR planar CDRPM.

## 4 Investigation of Kinematic Sensitivity of Redundant Robots

From the study conducted in [20], it reveals that when computing the kinematic sensitivity for redundant PM with respect to the $\infty$-norm constraint, the number of hyperplanes increases and further confines polyhedral of constraint which is sought at the outset. In fact appending redundant rows to the Jacobian matrix of the mechanism, will result into omission of farther vertices of constraint polyhedron and the mechanism kinematic sensitivity reduces significantly. The latter implies avoiding singular configurations within the workspace which can be regarded as a must for the design of a PMs. Using the pseudo-code of Table 3, one can determine the interval vertices of the hyperplanes in a redundant state. Once the interval vertices are generated with respect to the latter pseudo-code, the calculation of kinematic sensitivity is accomplished in the same way as the non-redundant PM explained in Section 3. The output of this function (interval vertices) are valid when the product of the rest of the Jacobian matrix rows and the computed vertices vector, is a subset of interval $[-1,1]$. For the reason of dependency in interval analysis this production may result in an interval which could be wider than actual interval. Thus instead of multiplying the intervals, it is recommended to multiply the midpoints of the intervals in order to validate the computed vertices. In the pseudo-code of Table 3, n and m represent respectively number of active joints and number of DOFs in workspace of robot.

Figures 6, 7 and 8 represent respectively point-displacement and rotational FKS of a redundant PM, in which the fixed and moving attachment points lies on squares encompassed by circles 1 and 5 meters. The inside green region has a kinematic sensitivity less than 0.3, $\sigma_d = 0.3$. It should be noted that, considering $\sigma_d = 0.35$, as the previous section leads to cover the whole workspace. From the latter, it can be concluded that in order to benefit from the whole workspace the kinematic sensitivity of the mechanisms under study should be equal to $\sigma_d = 0.35$. The foregoing

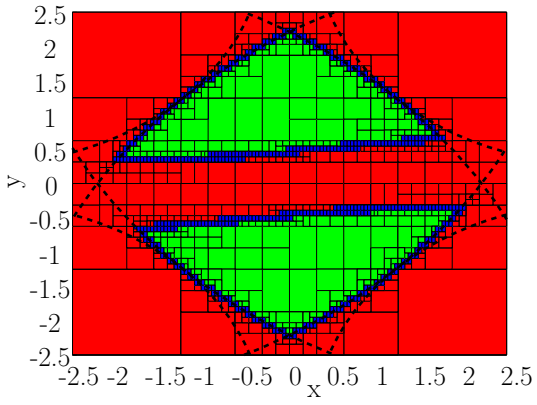


**Fig. 6** Point-displacement FKS, the inside (green) region, of a 4-RPR PM with $c = f = \infty$ and $\sigma_d = 0.35$ for $\phi = \frac{\pi}{6}$. The dashed lines represent the boundary of the workspace.

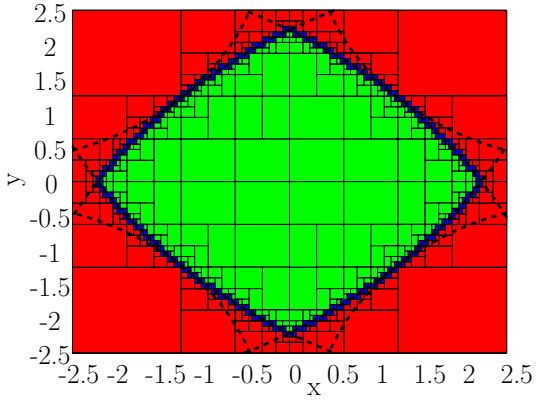


**Fig. 7** Rotational FKS, the inside (green) region, of a 4-RPR PM with $c = f = \infty$ and $\sigma_d = 0.35$ for $\phi = \frac{\pi}{6}$. The dashed lines represent the boundary of the workspace.

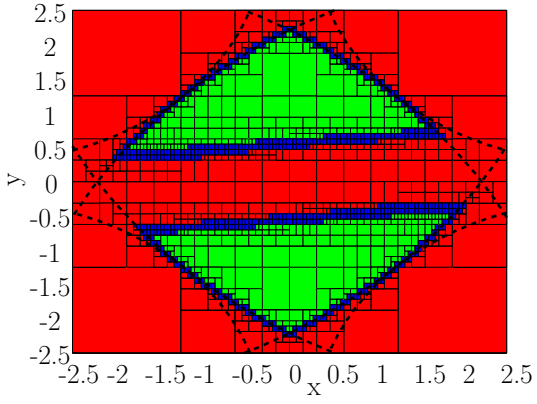


**Fig. 8** Point-displacement FKS, the inside(green) region, of a 4-RPR with $c = \infty$ and $f = 2$ and $\sigma_d = 0.3$ with $\phi = \frac{\pi}{6}$. The dashed lines represent the boundary of the workspace.

statement relates the workspace and design parameters to the kinematic sensitivity, a performance index, which open some avenues toward the optimum design of PM.

**Table 3** The Pseudo-code for the calculations of interval vertices of polyhedron of constraint in a redundant robot.

*Function:* Vertices=Compute-Vertex-Redundant([K])

```
t = 1
for j1 = 1 : n − (m − 1)
  for j2=j1 + 1 : n − (m − 2)
  ⋮
    for jm=jm−1 + 1 : n
      [Kn]=[[Kj1],[Kj2],...,[Kjm]]
      [Kw] = [K] without column [Kn]
      [KnVertices]=Compute-Vertex-Nonredundant([Kn])
      for 1:number of vertices of KnVertices
        [vertex]=each of vertices of KnVertices
        if −1 ≤ mid([Kw]) × mid([vertex]) ≤ 1
          vertices(t)=vertex
          t=t+1
        end
      end
    end
  ⋮
  end
end
```

## 5 Feasible Kinematic Sensitivity in CDRPMs

The unidirectional constraint imposed by cables causes the workspace analysis of CDRPMs to be always a crucial step in the design. As aforementioned, among several types of workspace introduced in the literature for CDRPMs, the controllable workspace is considered in this paper [26]. For controllable workspace analysis, the analytic method proposed in [29] is used. In this method a set of external wrenches is introduced and called *fundamental wrenches* in order to provide a physical interpretation of controllable workspace. Moreover, an analytical method is developed to determine the controllable workspace of redundant CDRPMs based on fundamental wrenches. The proposed method is generally applicable to any cable manipulators with any redundant cables as long as its Jacobian matrix is of full rank. The set of fundamental wrench for cable manipulator with one degree of redundancy refers to a set of $n+1$ vectors; each of them is equal to an opposite direction of column vector of Jacobian transpose as [29]:

$$\mathbf{A} = -\mathbf{J}^T = [\mathbf{A}_1|\mathbf{A}_2|...|\mathbf{A}_{n+1}]_{n\times(n+1)},\ \ \mathbf{w}_f = -\mathbf{A}_i,\ i = 1,...,n+1 \qquad (11)$$

In which $\mathbf{A}$ and $\mathbf{J}$ denote the structural and Jacobian matrix, respectively, and $\mathbf{w}_f$ is the fundamental wrench vector. According to the proposed theorem in [29], the controllable workspace can be obtained when all the determinant of the following matrix are positive.

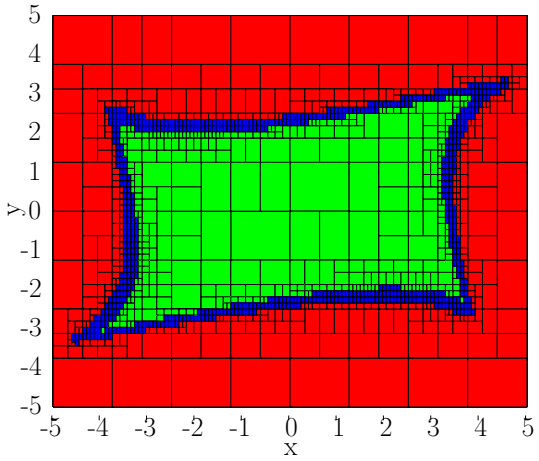


**Fig. 9** Controllable workspace, the green region, of a planar CDRPM with 4 cables.

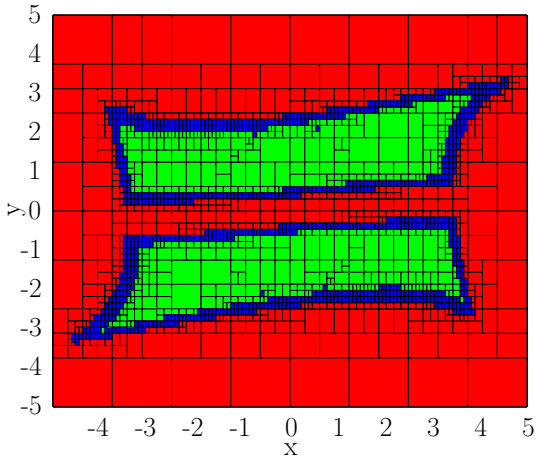


**Fig. 10** FKS, the green region, of a 4-RPR CDRPM with $c = \infty$ and $f = 2$ and $\sigma_d = 0.3$ with $\phi = \frac{\pi}{6}$.

$$\Delta_{ij} = \det[\mathbf{A}_1 ... \mathbf{A}_{j-1} \quad -\mathbf{w}_i \quad \mathbf{A}_{j+1} ... \mathbf{A}_{i-1} \mathbf{A}_{i+1} ... \mathbf{A}_{n+1}], i = 1, ..., n+1, i \neq j \qquad (12)$$

In the pseudo-code given in Table 5, the combination method to obtain the FKS controllable workspace is shown. The approach is similar to interval formulation of kinematic sensitivity in redundant manipulator, however, the constraint of controllable workspace is added at each iteration.

In Fig. 9, the inside (green) region illustrates the controllable workspace, while in Fig. 10, the inside (green) region represents the FKS workspace. In fact, this region is produced from blending controllable workspace and the area that has desired kinematic sensitivity, i.e. $\sigma_d = 0.3$. As it can be clearly seen from this figures, the interval analysis approach is capable to effectively combine two required kinematics characteristics in order to determine a suitable workspace for the robot. The volume of feasible kinematic sensitivity may be used as a suitable measure for optimal design of such manipulators. In order to compare the computational cost of

**Table 4** The proposed pseudo-code for the calculations of FKS controllable workspace of CDRPMs.

***Input***:$([x_t],[y_t],\phi,\varepsilon,\sigma_d)$
***Output***: $(L_{in},L_{out},L_{neg})$

$L \leftarrow ([x_t],[y_t])$
while $L \neq \emptyset$
  $[K]$=Compute-Jacobian-Matrix$([X],[Y],\phi)$
  $[V]$=Compute-Vertex- redundant$([K])$
  $[\Delta]$=Compute-all Delta's $([X],[Y],\phi)$
  **if** Feasible ($[V]$,$\sigma_d$) and all $\Delta$ are positive then
    $L_{in} \leftarrow ([X],[Y])$
  **else if** Out([V],$\sigma_d$) or one $\Delta$ is negative then
    Lout$\leftarrow ([X],[Y])$
  **else if** size$([X],[Y]) \geq \varepsilon$ then
    L $\leftarrow$ Bisect ($[X]$,$[Y]$)
  **else**
    $L_{neg} \leftarrow$ ($[X]$,$[Y]$)
  **end if**
**end while**

different methods, Table 4 summarizes the required time to calculate all the cases explained in the paper which are performed on a laptop computer with Core i7 CPU and 1.6GHz clock time. As it is seen in this table, the most time consuming method is to determine FKS workspace. Although the computations time is suitable for one time analysis of a given structure, if this method is to be used in an iterative optimization routine, the computational cost will be the major limitation, and should be significantly reduced. Current research is conducted to develop a suitable index for such optimization routine, and to reduce the computational cost.

**Table 5** Computation time for the calculation of various kinematic sensitivity indices, for all cases $c = 2$.

| Robot type | Kinematic sensitivity | norm of $f$ | $\varepsilon$ | Search area | Computation time (sec) |
|---|---|---|---|---|---|
| 3-R$\underline{\text{P}}$R | Point-displacement | $\infty$ | 0.05 | 6.25 | 764 |
| 3-R$\underline{\text{P}}$R | Rotational | $\infty$ | 0.05 | 6.25 | 418 |
| 3-R$\underline{\text{P}}$R | Point-displacement | 2 | 0.05 | 6.25 | 1348 |
| 4-R$\underline{\text{P}}$R | Point-displacement | $\infty$ | 0.05 | 6.25 | 815 |
| 4-R$\underline{\text{P}}$R | Rotational | $\infty$ | 0.05 | 6.25 | 513 |
| 4-R$\underline{\text{P}}$R | Point-displacement | 2 | 0.05 | 6.25 | 1128 |
| CDRPM | Feasible kinematic sensitivity | $\infty$ | 0.1 | 25.0 | 1783 |

## 6 Conclusions

This paper proposed a framework for the computation of feasible kinematic sensitivity, a more practical constant-orientation workspace in which the kinematic sensitivity is less than a given value, by means of interval analysis. The feasible kinematic sensitivity for both point-displacement and rotation motion was explored. From the previous studies conducted on kinematic sensitivity, a judicious combination of the norms were used to express accurately the function and constraint expressions of the optimization problem corresponding to the kinematic sensitivity analysis. For the workspace of planar PMs the constant-orientation workspace was used, while in the case of CDPMs, the controllable workspace was considered. As it is discussed in the paper, for a given design, a minimum feasible kinematic sensitivity value can be associated for which it can cover the whole workspace. Thus, ongoing works of this study includes to use of the minimum feasible kinematic sensitivity, set by the designer, as an optimization criteria to the end of optimum synthesis of the mechanism for which the minimum feasible kinematic sensitivity is known.

## References

1. G. Barrette and C. Gosselin, "Determination of the dynamic workspace of cable-driven planar parallel mechanisms," *Journal of Mechanical Design*, vol. 127, p. 242, 2005.
2. P. Cardou, S. Bouchard, and C. Gosselin, "Kinematic-sensitivity indices for dimensionally nonhomogeneous jacobian matrices," *IEEE Transactions on Robotics*, vol. 26, no. 1, pp. 166–173, 2010.
3. L. Dominjon, J. Perret, and A. Lécuyer, "Novel devices and interaction techniques for human-scale haptics," *The Visual Computer*, vol. 23, no. 4, pp. 257–266, 2007.
4. I. Ebert-Uphoff and P. Voglewede, "On the connections between cable-driven robots, parallel manipulators and grasping," in *proceedings of the IEEE International Conference on Robotics and Automation, ICRA'04.*, vol. 5, 2004, pp. 4521–4526.
5. A. Fattah, S. Agrawal *et al.*, "On the design of cable-suspended planar parallel robots," *Journal of Mechanical Design*, vol. 127, p. 1021, 2005.
6. Z. Geng and L. Haynes, "kinematic configuration of a stewart platform and its application to six degree of freedom pose measurements," *Robotics and Computer-Integrated Manufacturing*, vol. 11, no. 1, pp. 23–34, 1994.
7. S. Hamid and N. Simaan, "Design and synthesis of wire-actuated universal-joint wrists for surgical applications," in *proceedings of the IEEE International Conference on Robotics and Automation, ICRA'09.*, 2009, pp. 1807–1813.
8. F. Hao and J. Merlet, "Multi-criteria optimal design of parallel manipulators based on interval analysis," *Mechanism and machine theory*, vol. 40, no. 2, pp. 157–171, 2005.
9. T. Higuchi, A. Ming, and J. Jiang-Yu, "Application of multi-dimensional wire cranes in construction," in *proceedings of the 5th International Symposium on Robotics in Construction (ISRC88)*, 1988, pp. 661–668.
10. M. Husty and C. Gosselin, "On the singularity surface of planar 3-rpr parallel mechanisms," *Mechanics Based Design of Structures and Machines*, vol. 36, no. 4, pp. 411–425, 2008.
11. L. Jaulin, *Applied interval analysis: with examples in parameter and state estimation, robust control and robotics*. Springer Verlag, 2001, vol. 1.
12. J. Merlet, "Interval analysis and robotics," *Robotics Research*, pp. 147–156, 2011.

13. ——, "Solving the forward kinematics of a gough-type parallel manipulator with interval analysis," *The International Journal of robotics research*, vol. 23, no. 3, pp. 221–235, 2004.
14. R. Moore, *Interval analysis*. Prentice-Hall Englewood Cliffs, NJ, 1966, vol. 60.
15. R. Moore, R. Kearfott, and M. Cloud, *Introduction to interval analysis*. Society for Industrial Mathematics, 2009.
16. T. Morizono, K. Kurahashi, and S. Kawamura, "Realization of a virtual sports training system with parallel wire mechanism," in *proceedings of the IEEE International Conference on Robotics and Automation, ICRA'97*, vol. 4, 1997, pp. 3025–3030.
17. D. Oetomo, D. Daney, B. Shirinzadeh, and J. Merlet, "Certified workspace analysis of 3RRR planar parallel flexure mechanism," in *proceedings of the IEEE International Conference on Robotics and Automation, ICRA'08*, 2008, pp. 3838–3843.
18. G. Rosati, P. Gallina, and S. Masiero, "Design, implementation and clinical tests of a wire-based robot for neurorehabilitation," *IEEE Transactions on Neural Systems and Rehabilitation Engineering*, vol. 15, no. 4, pp. 560–569, 2007.
19. S. Rump, *Intlab-interval laboratory*. Citeseer, 1998.
20. M. Saadatzi, M. Masouleh, H. Taghirad, C. Gosselin, and P. Cardou, "Geometric analysis of the kinematic sensitivity of planar parallel mechanisms," *Transactions of the Canadian Society for Mechanical Engineering*, vol. 35, no. 4, p. 477, 2011.
21. ——, "On the optimum design of 3-RPR parallel mechanisms," in *proceedings of the 19th Iranian Conference on Electrical Engineering, ICEE'11*, 2011, pp. 1–6.
22. M. Saadatzi, M. Tale Masouleh, H. Taghirad, C. Gosselin, and M. Teshnehlab, "multi-objective scale independent optimization of 3-rpr parallel mechanisms," *Proceedings of the IFToMM*, 2011.
23. J. Salisbury and J. Craig, "Articulated hands," *The International Journal of Robotics Research*, vol. 1, no. 1, pp. 4–17, 1982.
24. Y. Su, B. Duan, R. Nan, and B. Peng, "Development of a large parallel-cable manipulator for the feed-supporting system of a next-generation large radio telescope," *Journal of Robotic Systems*, vol. 18, no. 11, pp. 633–643, 2001.
25. S. Tadokoro, R. Verhoeven, M. Hiller, and T. Takamori, "A portable parallel manipulator for search and rescue at large-scale urban earthquakes and an identification algorithm for the installation in unstructured environments," in *proceedings of the International Conference on Intelligent Robots and Systems, IROS'99*, vol. 2, 1999, pp. 1222–1227.
26. R. Verhoeven and M. Hiller, "Estimating the controllable workspace of tendon-based stewart platforms," *Advances in Robot Kinematics*, pp. 277–284, 2000.
27. R. Williams II, J. Albus, and R. Bostelman, "3D cable-based cartesian metrology system," *Journal of Robotic Systems*, vol. 21, no. 5, pp. 237–257, 2004.
28. T. Yoshikawa, "Analysis and control of robot manipulators with redundancy," in *proceedings of the First International Symposium Robotics Research*. Mit Press Cambridge, MA, 1984, pp. 735–747.
29. A. Zarif Loloei and H. Taghirad, "Transactions of the canadian society for mechanical engineering," Submitted to, March 2012.